Analytica Chimica Acta 1064 (2019) 65–70

Contents lists available at ScienceDirect

Analytica Chimica Acta

journal homepage: www.elsevier.com/locate/aca

A rapid MS/MS method to assess the deuterium kinetic isotope effect and associated improvement in the metabolic stability of deuterated biological and pharmacological molecules as applied to an imaging agent

Rhys B. Murphy [1], Naomi A. Wyatt, Benjamin H. Fraser, Nageshwar R. Yepuri, Peter J. Holden, Andrew T.L. Wotherspoon[*, 1], Tamim A. Darwish[**]

Australian Nuclear Science and Technology Organisation, Locked Bag 2001, Kirrawee DC, NSW, 2232, Australia

HIGHLIGHTS

- A simple *in vitro*/MS technique elucidates improved metabolic stability of deuterated analogues of drugs or biomolecules.
- Provides a rapid assessment whether the location of deuteration has a favourable or negligible impact on metabolic profile.
- A kinetic isotope effect was observed for the PET imaging agent PBR111 with deuteration at the 1,3-fluoropropoxy positions.
- A comparator study demonstrated a ~50% improvement in the primary pharmacokinetic data for 1,3-fluoropropoxy deuteration.

GRAPHICAL ABSTRACT

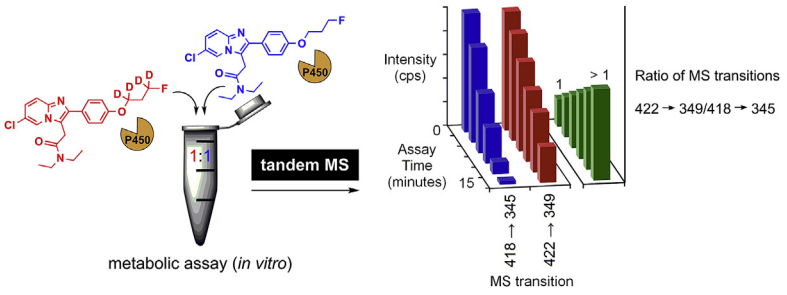

ARTICLE INFO

Article history:
Received 3 December 2018
Received in revised form
11 February 2019
Accepted 18 February 2019
Available online 22 February 2019

Keywords:
Deuteration biomolecules
Tandem mass spectrometry
Kinetic isotope effect
Microsomal assay
Organic synthesis
Metabolic stability

ABSTRACT

The deuterium kinetic isotope effect has been known for a period of 40 years, but it is only relatively recently that new drug entities (NDEs) incorporating deuterium demonstrating beneficial pharmacokinetics, pharmacodynamics, and toxicology have arrived to market. Determination of the precise location to deuterate and subsequently any evaluation for a kinetic isotope effect (KIE) is challenging. Typically, such an evaluation would be performed in an *in vitro* metabolic assay (e.g. liver microsomes) in separate reaction media for both the deuterated and non-deuterated analogues. Here, we have devised an approach whereby we incubate a 1:1 ratio of both the deuterated and protio-form of an imaging agent together in the same liver microsomal assay and determine the relative rate of consumption of both moieties, based upon specific MS-MS transitions unique to both molecules without the need for liquid chromatography-mass spectrometry (LC-MS) separation and quantification. Any deviation of the ratio of the MS transitions from the initial starting point indicated an observable KIE.

A site specific deuteration of PBR111, a neuroinflammation imaging agent, was chosen for a proof-of-concept study. Based upon prior mechanistic knowledge of PBR111, two locations were selected for

* Corresponding author.
** Corresponding author.
E-mail addresses: andrew.wotherspoon@sydney.edu.au (A.T.L. Wotherspoon), Tamim.Darwish@ansto.gov.au (T.A. Darwish).
[1] Equal first author.

https://doi.org/10.1016/j.aca.2019.02.025

deuteration; an active and inactive site, to corroborate that there was no significant KIE for the inactive site and confirm the efficacy of the developed methodology.

1. Introduction

The deuterium kinetic isotope effect (DKIE) is well known to improve the metabolic stability of molecules, with the C—D bond calculated to be between six and ten times stronger than a C—H bond [1]. Largely, the primary goal of any deuteration is to reduce the dose regimen of the drug (i.e. increase the biological longevity in comparison to the protio-variant). There is significant interest in both the progress of deuteration chemistry and applications of deuteration, evidenced by a number of reviews in the last decade [2–4] including back to back reviews in 2018 [5,6]. The pharmaceutical industry continues to examine the deuteration of drugs [3,7–10], and the world's first deuterated drug, deutetrabenazine (Fig. 1), was approved by the U.S. Food and Drug Administration in 2017 [11].

Deuterated drug candidates in clinical trial stages have been recently highlighted [12]. Selected examples include dextromethorphan-d_6 (several phase 2 studies, entered phase 3 studies [13–15]) and pentoxifylline-d_5 (completed a phase 2 study [16]) (Fig. 1).

Gillette [17] and Nelson [18] have developed a series of theoretical equations to explain any observed KIE governing the formation of metabolite products with P450 enzyme media from a substrate. These equation models are useful for predicting the precise kinetic mechanism for the P450 enzymatic isotope effect, but are procedurally involved, as determination of whether or not mechanistically a “parallel-pathway”, “non-dissociative” or “dissociative” pathways exists requires both competitive and non-competitive experimental assays of the protio/deutero substrates be performed. Moreover the level of complexity increases with the number of enzymes involved.

Furthermore, a number of examples of deuterated medical imaging agents (radiotracers) report increased metabolic stability [19–28], reportedly achieving:

- increased availability at the target [19,20],
- resistance to oxidation [19,20,24],
- higher signal-to-background contrast and detection sensitivity of positron emission tomography (PET) [20]
- reduced skull bone uptake of radioactivity [21,25],
- reduced trapping in tissues [22,26],
- reduced clearance favouring a particular metabolic pathway [23,27,28].

Prior knowledge of the metabolic fate of molecular entities can help inform the decision of suitable candidate sites to deuterate within the structure and thereby achieve the anticipated aim of enhancing metabolic stability. In the case of new or less studied molecules, even with *a priori* structure-activity pharmacological response information, the selection of the site for deuteration to gain a metabolically favourable outcome may be difficult [29]. For example, in an impressive body of work involving organic synthesis, radiochemistry, and *in vivo* biodistribution studies and PET imaging in rats, a deuterated serotonin transporter imaging agent unfortunately showed no difference relative to the non-deuterated *in vitro* or *in vivo* [30].

Deuterated analogues have been used principally as internal standards to aid in quantitative serum/plasma measurements of prescription and illicit drugs [31,32]. Only relatively recently has there been a concerted effort to examine the impact of deuteration to improve the pharmacology of existing and new drug entities via the DKIE. Owing to the fact the physical chemistry of the deutero-variant is identical, determination of any improved metabolic or pharmacokinetic profile proceeds with two or more separate assays. In the case of gradient high pressure liquid chromatography (HPLC), radiolabelling can assist in quantitation as the parent and metabolites quantitation will be more or less unaltered by the polarity/compositional impact on the chromophore [33]. However, radiolabelling requires an additional step and presupposes the radiolabel does not alter the metabolism and the metabolites still retain the radiolabel for quantitation, which is not always the case [33]. Although radiolabelling can provide accurate quantitative data of the NDE, this does not negate the need for two independent comparative assays to be performed. In the case of radiolabelling, there are a number of added complexities including facilities and infrastructure for the production and provision of the radioisotope, time-critical chemical synthesis, purification, testing upon radiolabelling, with designated and specialist equipment associated with radioanalysis and safety precautions.

Given the primary interest is to determine the impact of deuteration to induce a KIE, if any, we thought we'd incorporate both isotopologues simultaneously and relate any alteration in metabolic rate to a measured change in the ratio of mass-spectral transitions unique to both analogues in the same assay. This removes any possibility of instrument bias (arising from drift over the duration of carrying out two separate assays), since both analogues are present in the same quenched medium and any error associated with the accuracy of pipette dispensing of microsomal media components and quenching agent.

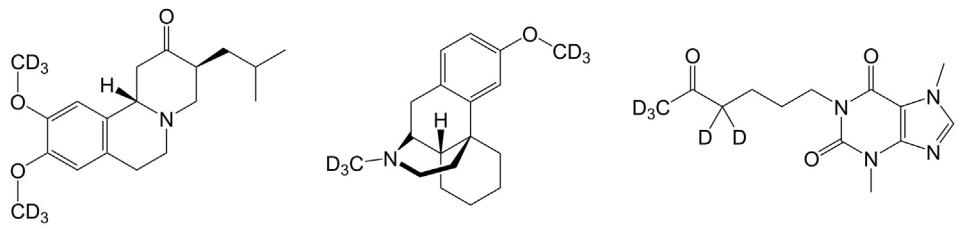

deutetrabenazine (AUSTEDO) dextromethorphan-d_6 pentoxifylline-d_5

Fig. 1. Selected deuterated drugs at various stages of approval and clinical trials.

The work reported in this study should not be confused with the application and use of deuterated internal standards for quantitative measurement of drugs of illicit or prescribed use. Furthermore, the methodology differs from the use of deuterated and other stable isotopes as tracers to characterise challenging metabolites as a result of few structurally informative fragment ions in LC-MS/MS spectra [34,35]. While our method cannot provide the level of mechanistic detail as methods of Gillette [17] and Nelson [18], this degree of characterisation would involve measurements of individual enzymes, and measurements of metabolites. The approach herein should inform whether such in-depth kinetic assays are warranted. As such, it should be viewed as gleaning in an expedient and simple approach, via a 'one-pot' assay, the best estimate of $(k_H/k_D)_{obs}$ and an indication of potential *in vivo* host metabolism. Furthermore, in the approach we have undertaken, we demonstrate that it is not always necessary to perform a prior liquid chromatographic separation before tandem mass spectrometric measurement of both deuterated and protio-moieties [29,36] – a direct syringe infusion will suffice.

Previous work done in our laboratories with the radiotracer [^{18}F]PBR111-H (compound **1**, Fig. 1), a translocator protein (TSPO) ligand primarily used for imaging neuroinflammation [37,38], has shown that this molecule is rapidly metabolised at the aliphatic propyl side chain containing the fluorine radiolabel, eventually yielding free fluorine, which is taken up by bone [39]. Combined, the other two principal metabolic clearance pathways (e.g. *N*-dealkylation or hydroxylation) constitute no greater than 40% of the metabolite total [39].

Based upon this metabolic data, we have examined specifically the efficacy of deuteration on the propyl side chain to reduce the generation of free fluorine [40]. [^{18}F]PBR111-d_4(propyl) (compound **2**, Fig. 2), exhibits slower metabolic breakdown and a decreased rate of formation of polar metabolites *in vitro* (rat and human liver microsomes) relative to the non-deuterated variant [39,40].

Liver microsomes contain a mixture of drug metabolising enzymes (including cytochrome P450s) and are used to study drug metabolism. Using a rat liver microsome assay (based on our previous work on PBR111 [39], with some minor adjustments, detailed in A1), we subjected an initially 1:1 mixture of protio- PBR111 (PBR111-H, compound **1**) relative to two independent deuterated variants, PBR111-d_4(propyl) (compound **2**) or PBR111-d_4(ring) (compound **3**), to *in vitro* metabolism over 15 min. We examined the dominant MS/MS transition ratio for this 1:1 mixture of deuterated and non-deuterated PBR111 at different time points during the assay.

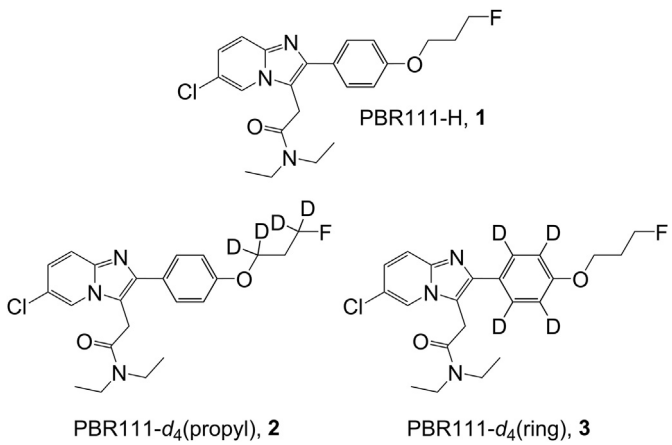

Fig. 2. PBR111-H, compound **1**, and its deuterated analogues PBR111-d_4(propyl) and PBR111-d_4(ring), compounds **2** and **3** respectively.

2. Materials and methods

2.1. Materials

The synthesis of PBR111-H (compound **1**) has been previously reported [38]. PBR111-d_4(propyl) (compound **2**) was synthesised with overall 99 ± 2% deuterium incorporation in the 1,3-propyl positions (A6-A7). In summary, deuteration of the 1,3-propyl chain was achieved by $LiAlD_4$ reduction of diethyl malonate to afford 1,3-propanediol-d_4 (compound **14**, A6.1). Subsequent mono-PMB protection then bromination afforded compound **16** (A6.3), which was coupled via the bromine terminus to the phenolic moiety of the pyridineimidazole core of literature compound **13b** [38]. The PMB group in compound **17** (A7.1) was replaced with Ts (compound **19**, A7.3) and fluorinated by using TBAF (A7.4). PBR111-d_4(ring) (compound **3**) was synthesised with overall 97 ± 2% deuterium incorporation on the *p*-substituted phenyl ring (A3-A4). In summary, deuteration of the phenyl ring in PBR111 was achieved by using phenol-d_6 (98%, Cambridge Isotope Laboratories, DLM-370-5) to first synthesise 2-bromo-4′-methoxyacetophenone-d_4 (compound **6**, A3.3, three steps), the starting material required for the literature synthesis of PBR111-H [38]. To avoid almost quantitative back-exchange of deuterium with hydrogen *ortho*-to the phenyl oxygen substituent under harsh acidic conditions for a late-stage precursor using the literature method for this compound [38] (i.e. conversion of compound **10**, A4.4, to compound **12**, A4.6), it was necessary to undertake two separate reactions; base hydrolysis of the primary amide in compound **10** to the carboxylic acid in compound **11** [41] (A4.5), followed by BBr_3-mediated ether demethylation [40] to afford compound **12** (A4.6).

The full synthesis and characterisation data for PBR111 compounds **2**–**3** and their precursors are provided in the appendix (A3-A8). The HPLC of PBR111 compounds **1**–**3** are provided in the appendix (A9).

2.2. Methods

2.2.1. Liver microsome assay

The experimental details for the liver microsome assay (modified from previous work [39] to suit the mixture of PBR111-d_4/PBR111-H used in this work) are provided in full in A1.

2.2.2. Instrumental analysis

An AB SCIEX QTRAP 4000 MS/MS with an ESI source was used with the following parameters: N_2 curtain gas = 20; collisionally activated dissociation = medium; ion spray voltage = 5000; temperature of ion source = 0; nebulising gas = 50; drying gas = 50; ion source heater = ON; declustering potential = 90; entrance potential = 10; collision energy = 40; collision cell exit potential = 15. Data acquisition and processing used the Analyst software package (version 1.5.2). We directly infused the validation standards and metabolised samples using a syringe pump at a flow rate of 10 μL min^{-1} (Harvard Apparatus 11 Plus syringe pump). The aliquots of validation standard or microsomal-incubated PBR111-d_4/PBR111-H (200 μL) isolated at the time points indicated in A1, were quenched with acetonitrile (200 μL) and subsequently diluted with a 1:1 acetonitrile/H_2O/0.05% formic acid solution (1.8 mL) to ensure adequate ionisation. Samples (2.0 mL) were pre-filtered (0.45 μM PTFE, Phenomenex Phenex AFO-3102-52), and directly infused for a period of 10 min prior to data acquisition. Data was acquired (in triplicate) over a period of 0.8–1 min for each sample/validation standard. The specific transitions (to ensure analyte selectivity) for the deuterated and non-deuterated molecules were as follows: *m*/*z* 422 → 349 for PBR111-d_4 and 418 → 345 PBR111-H, corresponding with intact molecule and the MS-induced fragment for loss of

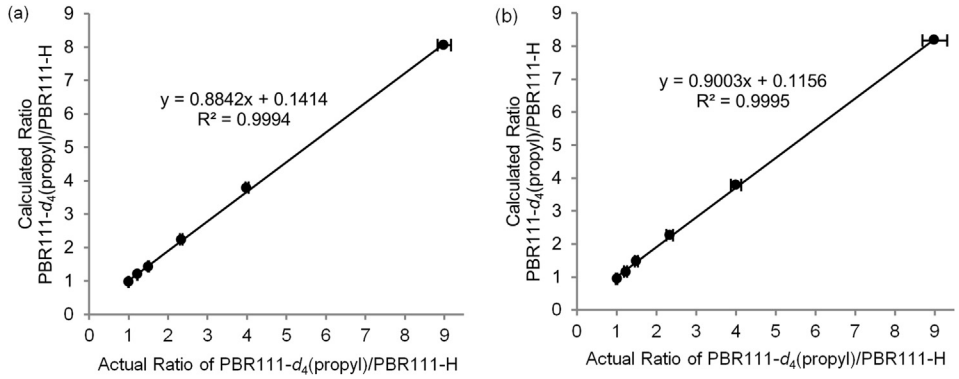

Fig. 3. Calibration curve for the actual and calculated ratios of PBR111-d_4(propyl)/PBR111-H (N = 1, error bars are ±1 SD) at an overall concentration of (a) 11.5 μM, and (b) 1.15 μM (graphs constructed from raw data in A11).

$N(CH_2CH_3)_2$ from the amide pendant to the imidazo[1,2-*a*]pyridine ring (A10) associated with each molecular analogue. For PBR111, our previous work [39] informed us of the fragmentation of intact parent compound, as well as metabolites and associated fragmentations. A full listing of the transitions associated with each molecule can be found in A10, along with acquisition parameters. The counts per second (cps) for the transitions were averaged over 0.1–0.45 min per data collection. The ratio of the cps for 422 → 349 relative to 418 → 345 was calculated. For the validation standards (see below), the % RSD of the ratio was 1–4% (A11). The transition 422 → 349/418 → 345 was selected as it was of sufficient intensity at the low concentrations of intact PBR111 following the liver microsome assay. However, any pair of analogous transitions arising from the intact compound can be chosen for analysis provided (a) the ratio of the intensity of the transitions is linear with concentration, and (b) the pair of transitions is of sufficient intensity to be quantified at each time point of the microsome assay. We have provided this data for other pairs of analogous transitions in the supporting information (A12, A14). A solution of 1:1 acetonitrile:H_2O (0.05% formic acid) was used to clean the MS between different samples. The transitions of interest were monitored for return to low cps (approx. 50 cps, 30–60 min at a flow rate of 30 μL min^{-1}) before measuring the next sample to ensure correct sample readings.

2.2.3. Statistical analysis

Statistical analysis (one-way ANOVA using the XLSTAT add-in for Microsoft Excel) was undertaken on the means of the ratio for each of the six time points in the metabolic assay of PBR111-d_4/PBR111-H. The mean of the ratio at different time points was calculated from triplicate assays, with each individual assay time point also measured in triplicate.

3. Results and discussion

3.1. Validation and quality assurance

To ensure there were no or minimal interferences from the sample matrix we injected via the syringe pump, the diluted sample matrix comprising of the microsomal assay medium (liver microsomes, glucose 6-phosphate (G6P), G6P dehydrogenase, nicotinamide adenine dinucleotide phosphate (NADP), phosphate buffer) and the MS diluent (1:1 acetonitrile/H_2O/0.05% formic acid). PBR111 was not included in this method blank. Although some signal was noted to be observed for the respective transitions of both compounds (418 → 345 and 422 → 349), each registered less than 25 cps, yielding a proposed limit of detection (LOD) of ~13 nM and limit of quantitation (LOQ) of ~130 nM of each parent compound. The analysis of known ratios of PBR111-d_4(propyl)/PBR111-H (prepared in ratios of 90:10, 80:20, 70:30, 60:40, 55:45, 50:50) in a series of calibration standards (containing phosphate buffer and overall 11.5 μM[2] PBR111 mixture, but excluding the microsomal assay medium) was undertaken to ensure linearity in response. The calibration standard was diluted as per the assay conditions. Additionally, each calibration standard was diluted a further tenfold, to simulate the concentration of intact tracer encountered post-metabolism. The two ascending and descending ratios of PBR111-d_4(propyl)/PBR111-H for the calibration spanned replica assay concentrations of 0.12–10.4 μM PBR111 (essentially 1–200% intact tracer). The ratio of the counts per second (cps) of the analogous MS/MS transitions for PBR111-d_4(propyl) versus PBR111-H were then calculated from the experimental data and compared with the actual ratios (raw data is provided in A11). Fig. 3 (a) and (b) are the associated calibration curves of the actual and calculated ratios of PBR111-d_4(propyl)/PBR111-H, and display excellent linearity ($R^2 \geq 0.999$) across the ratios and concentration ranges examined. The ionisation efficiency and internal fragmentation energy of PBR111-H and PBR111-d_4(propyl) appear to be similar,

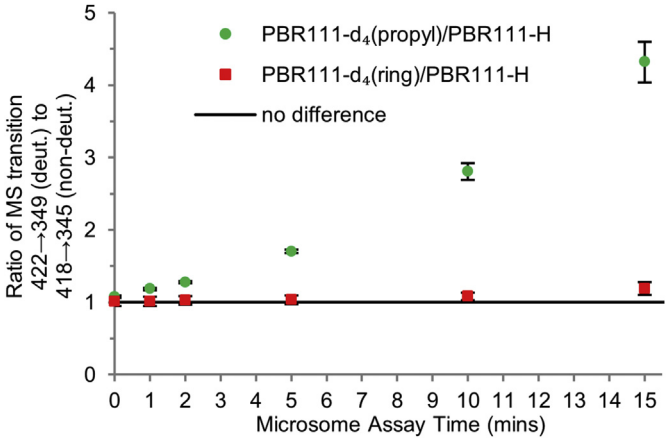

Fig. 4. Relative metabolic stability *in vitro* (rat liver microsomes) of PBR111-d_4 to PBR111-H, for deuteration of the propyl chain and phenyl ring. A positive deviation with time from the starting ratio indicates increased metabolic stability (N = 3, error bars are ±1 SE).

[2] 10 μM overall PBR111 mixture (1:1 PBR111-d_4/PBR111-H) was used for the liver microsome assay.

Table 1
Summary of pharmacokinetic parameters for PBR111-H and PBR111-d_4(propyl).

Compound	k (min^{-1})	$t_{1/2}$ (min)	AUC ((μg.min)mL^{-1})	N_{15}[a]	Ratio[b]
PBR111-H, **1**	0.27	2.57	8.29	0.037	3.88
PBR111-d_4(propyl), **2**	0.18	3.85	12.29	0.14	

[a] Quantity remaining after 15 min, starting from an initial quantity of 2.09 μgmL^{-1} (5 μM) of PBR111-H and 2.11 μgmL^{-1} (5 μM) PBR111-d_4(propyl), calculated using the half-life exponential decay equation, $N_t = N_0\left(\frac{1}{2}\right)^{\frac{t}{t_{1/2}}}$.

[b] Ratio of quantity of PBR111-d_4(propyl) to PBR111-H remaining after 15 min based on their respective half-lives.

based on the data for the 1:1 mixture and measurement of the ratio of 422 → 349 to 418 → 345.

3.2. Evaluation of deuterium KIE upon PBR111

After confirming the methodology for determining the ratio was free of interferences and offered sufficient sensitivity, robustness, and linearity, the MS method was applied to the metabolic assay using liver microsomes and the 1:1 PBR111-d_4(propyl)/PBR111-H mixture (A1, assay done in triplicate). The assay samples were run in order of increasing concentration (15 min assay time point run first, starting time point run last).

The ratio of the MS transitions for 422 → 349 to 418 → 345 revealed substantial deviation from the starting ratio with assay time for PBR111-d_4(propyl) (Fig. 4, green circles), indicating the metabolic stability of PBR111-d_4(propyl) is greater than that of PBR111-H. This is in line with the results from our previous work [39,40] where the major metabolite for PBR111-H arises from cleavage of the fluoropropyl chain (*O*-dealkylated). To further demonstrate the utility of the method, PBR111-d_4(ring) was synthesised to be metabolised similarly to PBR111-H, as our previous work [39] had informed us that only a comparatively small amount of a ring hydroxylated metabolite is formed in comparison to the *O*-dealkylated metabolite. Applying the MS method, PBR111-d_4(ring)/PBR111-H (assay performed in triplicate) showed minimal deviation from the starting ratio with assay time for PBR111-d_4(ring) (Fig. 4, red squares), demonstrating PBR111-d_4(ring) is metabolised at a similar rate to PBR111-H, as expected given previous work [39]. This separate molecular entity demonstrates that introduction of deuterium on the phenyl ring does not increase the metabolic stability, as this moiety is not subject to significant metabolism by liver microsomes [39]. Furthermore, it seems likely that the relative ability for both PBR111-d_4(ring) and PBR111-H to generate $[M+H]^+$ is similar.

Statistical analysis was undertaken (one-way ANOVA; criteria: F-statistic > F-critical) and confirmed the means of the ratios across the six time points for PBR111-d_4(propyl)/PBR111-H are significantly different (F-statistic = 107.7, F-critical = 3.1, $\alpha = 0.05$, $p = 1.53 \times 10^{-9}$, $df = 17$). Conversely, the same test applied to PBR111-d_4(ring)/PBR111-H revealed the means of the ratios across the six time points are not significantly different (F-statistic = 1.1, F-critical = 3.1, $\alpha = 0.05$, $p = 0.41$, $df = 17$). These two tests established there is improved metabolic stability of PBR111-d_4(propyl) relative to PBR111-H, but not for PBR111-d_4(ring), as expected. While the ratio plot in Fig. 4 is a convenient way of demonstrating the data, the relative metabolic stability of PBR111-d_4 against PBR111-H can alternatively be represented without taking the ratio as the percent depletion (normalised) for each compound (derived from the cps for the MS transitions). This is shown in S13.

3.3. Pharmacokinetic parameters of PBR111-H and PBR111-d_4(propyl)

The PK microsomal metabolism data for PBR111-H and PBR111-d_4(propyl) was fitted to a one compartmental model with a corresponding R^2 of >0.998 determined for both molecules in a comparator study. The area under the curve (AUC) was calculated using the trapezoidal summation approach. The corresponding elimination rate constant (k), elimination half-life ($t_{1/2}$) and AUC are summarised in Table 1. Using the calculated half-life, it can be estimated that there would be 3.88 times as much PBR111-d_4(propyl) remaining after 15 min relative to PBR111-H (Table 1). This theoretical ratio is similar to the experimental ratiometric transition data presented in Fig. 4.

4. Conclusion

The MS/MS ratio method conveniently demonstrates the difference in metabolic stability *in vitro* between deuterated and non-deuterated isotopologues mixed simultaneously in a liver microsome assay. This was achieved by examining the change in the ratio of the analogous MS transitions of intact deuterated and non-deuterated molecules in multiple reaction monitoring (MRM) mode at different time points in the assay. As expected, when the site of deuteration assists with metabolic stability, the ratio of the transition relative to non-deuterated changes with assay time. When the site of deuteration does not greatly assist with metabolic stability, there is minimal change in the ratio of the same transition relative to non-deuterated. As the distinct mass (unique to each molecule) is being monitored (rather than the UV- or radiodetector in HPLC, where there is no independent measurand), there is no need to analyse the compounds independently. We suggest this MS/MS approach could be applied as a rapid screening tool for deuterated and non-deuterated analogues of other molecules, including pharmacologically active molecules, to aid in determining the suitability of the chosen site of deuteration. The methodological approach can also be applied to cold radiotracers, as there is no radiolabelling requirement to use this method.

Conflicts of interest

There are no conflicts to declare.

Declaration of interests

The authors declare that they have no known competing financial interests or personal relationships that could have appeared to influence the work reported in this paper.

Acknowledgements

The National Deuteration Facility thanks the NSW Government for the provision of a Research Attraction and Acceleration Program grant to the Australian Nuclear Science and Technology Organisation. The National Deuteration Facility is partly supported by the National Collaborative Research Infrastructure Strategy – an initiative of the Australian Government.

Appendix A. Supplementary data

Supplementary data to this article can be found online at https://doi.org/10.1016/j.aca.2019.02.025.

References

[1] K.J. Laidler, Chemical Kinetics, Harper & Row, 1987.
[2] T.G. Gant, Using deuterium in drug discovery: leaving the label in the drug, J. Med. Chem. 57 (9) (2014) 3595–3611.
[3] G.S. Timmins, Deuterated drugs: where are we now? Expert Opin. Ther. Pat. 24 (10) (2014) 1067–1075.
[4] J. Atzrodt, et al., The renaissance of H/D exchange, Angew. Chem. Int. Ed. 46 (41) (2007) 7744–7765.
[5] J. Atzrodt, et al., Deuterium- and tritium-labelled compounds: applications in the life sciences, Angew. Chem. Int. Ed. 57 (7) (2018) 1758–1784.
[6] J. Atzrodt, et al., C–H functionalisation for hydrogen isotope exchange, Angew. Chem. Int. Ed. 57 (12) (2018) 3022–3047.
[7] V. Uttamsingh, et al., Altering metabolic profiles of drugs by precision deuteration: reducing mechanism-based inhibition of CYP2D6 by paroxetine, J. Pharmacol. Exp. Therapeut. 354 (1) (2015) 43–54.
[8] S.L. Harbeson, et al., Altering metabolic profiles of drugs by precision deuteration 2: discovery of a deuterated analog of ivacaftor with differentiated pharmacokinetics for clinical development, J. Pharmacol. Exp. Therapeut. 362 (2) (2017) 359–367.
[9] G.S. Timmins, Deuterated drugs; updates and obviousness analysis, Expert Opin. Ther. Pat. 27 (12) (2017) 1353–1361.
[10] R.H. Howland, Deuterated drugs, J. Psychosoc. Nurs. Ment. Health Serv. 53 (9) (2015) 13–16.
[11] U.S. Food & Drug Administration, Drugs@FDA: FDA Approved Drug Products, AUSTEDO (DEUTETRABENAZINE), 2017, in: https://www.accessdata.fda.gov/scripts/cder/daf/index.cfm?event=overview.process&varApplNo=208082.
[12] C. Schmidt, First deuterated drug approved, Nat. Biotechnol. 35 (2017) 493.
[13] L. Nguyen, A.L. Scandinaro, R.R. Matsumoto, Deuterated (d6)-dextromethorphan elicits antidepressant-like effects in mice, Pharmacol. Biochem. Behav. 161 (2017) 30–37.
[14] Efficacy, Safety, and Tolerability of AVP-786 for the Treatment of Agitation in Patients with Dementia of the Alzheimer's Type, 2018. https://www.clinicaltrials.gov/ct2/show/NCT02442778.
[15] Assessment of the Efficacy, Safety, and Tolerability of AVP-786 (Deudextromethorphan Hydrobromide [d6-DM]/Quinidine Sulfate [Q]) for the Treatment of Agitation in Patients with Dementia of the Alzheimer's Type, 2018. https://clinicaltrials.gov/ct2/show/NCT03393520?term=avp-786&rank=5.
[16] A Phase 2 Study to Evaluate the Safety and Efficacy of CTP-499 in Type 2 Diabetic Nephropathy Patients, 2018. https://clinicaltrials.gov/ct2/show/NCT01487109?term=CTP-499&rank=3.
[17] J.R. Gillette, J.F. Darbyshire, K. Sugiyama, Theory for the observed isotope effects on the formation of multiple products by different kinetic mechanisms of cytochrome P450 enzymes, Biochemistry 33 (10) (1994) 2927–2937.
[18] S.D. Nelson, W.F. Trager, The use of deuterium isotope effects to probe the active site properties, mechanism of cytochrome P450-catalyzed reactions, and mechanisms of metabolically dependent toxicity, Drug Metab. Dispos. 31 (12) (2003) 1481.
[19] J. Leyton, et al., [^{18}F]Fluoromethyl-[1,2-$^{2}H_4$]-choline: a novel radiotracer for imaging choline metabolism in tumors by positron emission tomography, Cancer Res. 69 (19) (2009) 7721–7728.
[20] A. Challapalli, et al., Biodistribution and radiation dosimetry of deuterium-substituted ^{18}F-fluoromethyl-[1,2-$^{2}H_4$]choline in healthy volunteers, J. Nucl. Med. 55 (2) (2014) 256–263.
[21] L. Cai, et al., Synthesis and Evaluation of two ^{18}F-labeled 6-iodo-2-(4'-N,N-dimethylamino)phenylimidazo[1,2-a]pyridine Derivatives as prospective Radioligands for β-Amyloid in Alzheimer's disease, J. Med. Chem. 47 (9) (2004) 2208–2218.
[22] J.S. Fowler, et al., Selective reduction of radiotracer trapping by deuterium substitution: comparison of carbon-11-L-deprenyl and carbon-11-deprenyl-D2 for MAO B mapping, J. Nucl. Med. 36 (7) (1995) 1255–1262.
[23] Y.-S. Ding, et al., Mechanistic positron emission tomography Studies of 6-[^{18}F] Fluorodopamine in living baboon heart: selective Imaging and Control of radiotracer metabolism Using the deuterium isotope effect, J. Neurochem. 65 (2) (1995) 682–690.
[24] T.H. Witney, et al., Evaluation of deuterated ^{18}F- and ^{11}C-labeled choline analogs for cancer detection by positron emission tomography, Clin. Cancer Res. 18 (4) (2012) 1063–1072.
[25] M. Jahan, et al., Decreased defluorination using the novel beta-cell imaging agent [^{18}F] FE-DTBZ-d_4 in pigs examined by PET, EJNMMI Res. 1 (1) (2011) 33.
[26] S. Nag, et al., In vivo and in vitro characterization of a novel MAO-B inhibitor Radioligand, ^{18}F-labeled deuterated fluorodeprenyl, J. Nucl. Med. 57 (2016) 315–320.
[27] A. Kohen, H.-H. Limbach, Isotope Effects in Chemistry and Biology, cRc Press, 2005.
[28] D. Roston, Z. Islam, A. Kohen, Isotope effects as probes for enzyme catalyzed hydrogen-transfer reactions, Molecules 18 (5) (2013) 5543–5567.
[29] J. Schofield, et al., Effect of deuteration on metabolism and clearance of Neripsirdine (HP184) and AVE5638, Bioorg. Med. Chem. 23 (13) (2015) 3831–3842.
[30] F. Liu, et al., Deuterium-substituted 2-(2′-((dimethylamino)methyl)-4′-[^{18}F](fluoropropoxy)phenylthio)benzenamine as a serotonin transporter imaging agent, J. Labelled Comp. Rad. 61 (8) (2018) 576–585.
[31] T. Robin, et al., Fully automated sample preparation procedure to measure drugs of abuse in plasma by liquid chromatography tandem mass spectrometry, Anal. Bioanal. Chem. 410 (20) (2018) 5071–5083.
[32] M.K. Bjork, et al., Quantification of 31 illicit and medicinal drugs and metabolites in whole blood by fully automated solid-phase extraction and ultra-performance liquid chromatography-tandem mass spectrometry, Anal. Bioanal. Chem. 405 (8) (2013) 2607–2617.
[33] A.T. Wotherspoon, M. Safavi-Naeini, R.B. Banati, Microdosing, isotopic labeling, radiotracers and metabolomics: relevance in drug discovery, development and safety, Bioanalysis 9 (23) (2017) 1913–1933.
[34] S.C. Turfus, et al., Use of human microsomes and deuterated substrates: an alternative approach for the identification of novel metabolites of ketamine by mass spectrometry, Drug Metab. Dispos. 37 (8) (2009) 1769.
[35] J. Ni, et al., Characterization of benzimidazole and other oxidative and conjugative metabolites of brimonidine in vitro and in rats in vivo using on-line H/D exchange LC-MS/MS and stable-isotope tracer techniques, Xenobiotica 37 (2) (2007) 205–220.
[36] F. Wang, et al., Design, synthesis and biological evaluation of deuterated Vismodegib for improving pharmacokinetic properties, Bioorg. Med. Chem. Lett 28 (14) (2018) 2399–2402.
[37] S. Dedeurwaerdere, et al., PET imaging of brain inflammation during early epileptogenesis in a rat model of temporal lobe epilepsy, EJNMMI Res. 2 (1) (2012) 60.
[38] C.J.R. Fookes, et al., Synthesis and biological Evaluation of substituted [^{18}F] Imidazo[1,2-a]pyridines and [^{18}F]Pyrazolo[1,5-a]pyrimidines for the Study of the peripheral benzodiazepine receptor using positron emission tomography, J. Med. Chem. 51 (13) (2008) 3700–3712.
[39] S. Eberl, et al., Preclinical in vivo and in vitro comparison of the translocator protein PET ligands [^{18}F]PBR102 and [^{18}F]PBR111, Eur. J. Nucl. Med. Mol. Imaging 44 (2) (2017) 296–307.
[40] Naomi A. Wyatt, Mitra Safavi-Naeini, Andrew Wotherspoon, Andrew Arthur, An P. Nguyen, Arvind Parmar, Hasar Hamze, Charmaine M. Day, David Zahra, Lidia Matesic, Emma K. Davis, Gita L. Rahardjo, Nageshwar R. Yepuri, Rachael K. Shepherd, Rhys B. Murphy, Tien Q. Pham, Vu H. Nguyen, Paul D. Callaghan, Peter J. Holden, Marie-Claude Gregoire, Tamim A. Darwish, Benjamin H. Fraser, [18F]PBR111-d4 - An improved 2nd generation deuterated radiotracer for imaging inflammation, in: 12th Congress of the World Federation of Nuclear Medicine and Biology (WFNMB2018), Melbourne, Australia, 20-24 April, 2018 abstract/poster WFNMB18-ABS-1379.
[41] J. Lange, et al., A structure-activity relationship study of the affinity of selected imidazo[1,2-a]pyridine derivatives, congeners of zolpidem, for the ω_1-subtype of the benzodiazepine receptor 58 (2001) 43–52.